Contribution from the Department of Chemistry,
Harvard University, Cambridge, Massachusetts 02138

Metal Ion Exchange Reactions in Cage Molecules: The Systems $[M_{4-n}M'_n(SC_6H_5)_{10}]^{2-}$ (M, M' = Fe(II), Co(II), Zn(II), Cd(II)) with Adamantane-like Stereochemistry and the Structure of $[Fe_4(SC_6H_5)_{10}]^{2-}$

K. S. HAGEN, D. W. STEPHAN,[1] and R. H. HOLM*

Received March 2, 1982

The compound $(Me_4N)_2[Fe_4(SPh)_{10}]\cdot C_3H_7CN$ crystallizes in monoclinic space group $P2_1/n$ with $a = 14.314$ (3) Å, $b = 24.038$ (5), Å, $c = 22.101$ (3) Å, $\beta = 96.06$ (1)°, and $Z = 4$. On the basis of 5470 unique data ($I > 3\sigma(I)$) the crystal structure has been refined to $R = 4.1\%$. The structure of $[Fe_4(SPh)_{10}]^{2-}$ consists of a $Fe_4(\mu\text{-}S)_6$ cage of adamantane-like stereochemistry, distorted from idealized T_d symmetry. Coordination at each tetrahedral Fe(II) site is completed by a terminal benzenethiolate ligand. The four chair Fe_3S_3 rings of the cage have the 3-2-1-0 disposition of axial phenyl groups, rendering all ligands inequivalent in the solid state. The complex $[Fe_4(SPh)_{10}]^{2-}$ is the fifth example of $M_4(\mu\text{-}SR)_6$ adamantane-like stereochemistry, the most frequently encountered arrangement in metal-thiolate cage species. ^1H NMR studies of the series $[M_4(SPh)_{10}]^{2-}$, M = Fe(II), Co(II), Zn(II), Cd(II), have revealed rapid pyramidal inversion of μ-SPh ligands and the occurrence of two reactions. Each complex is stereochemically nonrigid owing to the occurrence of terminal $\leftrightarrow$ bridge ligand scrambling, for which a pathway is suggested. The systems $[M_4(SPh)_{10}]^{2-}/[M'_4(SPh)_{10}]^{2-}$, M/M' = Fe/Co, Co/Zn, Co/Cd, Fe/Zn, Fe/Cd, undergo rapid metal ion exchange resulting in the formation of mixed-metal species $[M_{4-n}M'_n(SPh)_{10}]^{2-}$ ($n = 1$-3), which are readily detected by their isotropically shifted ^1H NMR spectra. Equilibrium constants of the first three systems indicate approximately statistical product distribution. Several rough analogies are drawn between binding sites and metal ion substitution in adamantane-like cages and in the protein metallothionein. ^{113}Cd chemical shifts in the Zn/Cd system and in $[Cd(SPh)_4]^{2-}$ provide further evidence for the deshielded nature of the metal in $Cd(SR)_4$ units.

Introduction

The chemistry of metal thiolates has not as yet reached a stage of definition comparable to that of the metal alkoxides.[2] However, research in the last 15 years, and particularly in the last decade, has resulted in the emergence of a broad class of molecules that, as the alkoxides, encompass a substantial range of nuclearity and structural complexity. Metal thiolates are considered here to include those compounds which, if mononuclear, involve ligation by RS^- groups only and, if polynuclear, contain as skeletal bridging ligands these groups only. Examples range from a variety of mononuclear species $[M(SR)_4]^{2-,1-,0}$ [4-8] to penta- and hexanuclear complexes such as $[Cu_5(S\text{-}t\text{-}Bu)_6]^-$,[9] $[M^I_5(SPh)_7]^{2-}$,[10] and $[Ni_6(SR)_{12}]$[11] and to entities of higher nuclearity including $[Zn_8Cl(SPh)_{16}]^-$,[12] $[Cd_{10}(SCH_2CH_2OH)_{16}]^{4+}$,[13] and $[Ag_{12}(SPh)_{16}]^{4-}$.[14]

Inspection of the structures of $[M_x(SR)_y]^{z-}$ complexes with $x \geq 4$ reveals the existence of molecular cages in which bridging thiolate sulfur atoms and metal atoms each form recognizable polyhedra. This point has been made by Dance[10,14] in his description of cage polyhedra in the series $[M_x(SPh)_{x+2}]^{2-}$ (M = Cu(I), Ag(I); $x = 4$-6). To date the most frequent stereochemical pattern in polynuclear metal thiolates is $M_4(\mu\text{-}SR)_6$, which is illustrated in Figure 1. The structure is of the adamantane type, containing a tetrahedrally disposed set of metal atoms and an octahedron of bridging sulfur atoms with overall (idealized) T_d symmetry. This structural type has been established for $[M_4(SPh)_{10}]^{2-}$ (M = Fe(II),[15] Co(II),[16] Zn(II)[17]), $[Zn_4(SPh)_8Cl_2]^{2-}$,[18] $[Fe_4(SPh)_6Cl_4]^{2-}$,[19] and $[Zn_4(SPh)_8(MeOH)]_n$.[20]

In the $M_4(\mu\text{-}SR)_6$ and larger cage complexes the bridging ligands, although unconnected, may be conceptualized as small matrices of metal-binding sites, with any further coordination completed by terminal ligands. The situation may be likened to that of native metallothionein proteins,[21] which usually contain 6-7 Zn + Cd atoms bound to all 20 cysteinyl residues in a single polypeptide chain of 61 total residues.[22,23] Recent ^{113}Cd NMR results demonstrate that the Cd atoms are sequestered in polynuclear groups of 3 or 4 and are bound mainly or exclusively by cysteinate sulfur atoms.[24,25] Spectroscopic properties of Co(II)-[26] and Ni(II)-substituted[26b] proteins are consistent with tetrahedral $M(Cys\text{-}S)_4$ sites, some of which,

(1) National Science and Engineering Research Council of Canada/NATO Postdoctoral Fellow, 1980-1982.
(2) Bradley, D. C.; Mehrotra, R. C.; Gaur, D. P. "Metal Alkoxides"; Academic Press: New York, 1978. This statement excludes the well-developed chemistry of 1,1-dithiolates[3a] and 1,2-dithiolates (dithiolenes[3b]).
(3) (a) Coucouvanis, D. *Prog. Inorg. Chem.* **1970**, *11*, 233; **1979**, *26*, 301. (b) McCleverty, J. A. *Ibid.* **1968**, *10*, 49.
(4) Lane, R. W.; Ibers, J. A.; Frankel, R. B.; Papaefthymiou, G. C.; Holm, R. H. *J. Am. Chem. Soc.* **1977**, *99*, 84.
(5) Holah, D. G.; Coucouvanis, D. *J. Am. Chem. Soc.* **1975**, *97*, 6917.
(6) Swenson, D.; Baenziger, N. C.; Coucouvanis, D. *J. Am. Chem. Soc.* **1978**, *100*, 1932.
(7) Coucouvanis, D.; Swenson, D.; Baenziger, N. C.; Murphy, C.; Holah, D. G.; Sfarnas, N.; Simopoulos, A.; Kostikas, A. *J. Am. Chem. Soc.* **1981**, *103*, 3350.
(8) Otsuka, S.; Kamata, M.; Hirotsu, K.; Higuchi, T. *J. Am. Chem. Soc.* **1981**, *103*, 3011.
(9) Dance, I. G. *J. Chem. Soc., Chem. Commun.* **1976**, 68.
(10) Dance, I. G. *J. Chem. Soc., Chem. Commun.* **1976**, 103; *Aust. J. Chem.* **1978**, *31*, 2195.
(11) Woodward, P.; Dahl, L. F.; Abel, E. W.; Crosse, B. C. *J. Am. Chem. Soc.* **1965**, *87*, 5251. Gould, R. O.; Harding, M. M. *J. Chem. Soc. A* **1970**, 875.
(12) Dance, I. G. *J. Chem. Soc., Chem. Commun.* **1980**, 818.
(13) Strickler, P. *Chem. Commun.* **1969**, 655.
(14) Dance, I. G. *Inorg. Chem.* **1981**, *20*, 1487.
(15) Hagen, K. S.; Berg, J. M.; Holm, R. H. *Inorg. Chim. Acta* **1980**, *45*, L17.
(16) Dance, I. G.; Calabrese, J. C. *J. Chem. Soc., Chem. Commun.* **1975**, 762. Dance, I. G. *J. Am. Chem. Soc.* **1979**, *101*, 6264.
(17) Hencher, J. L.; Khan, M.; Said, F. F.; Tuck, D. G. *Inorg. Nucl. Chem. Lett.* **1981**, *17*, 287.
(18) Dance, I. G. *Inorg. Chem.* **1981**, *20*, 2155.
(19) Coucouvanis, D.; Kanatzidis, M.; Simhon, E.; Baenziger, N. C. *J. Am. Chem. Soc.* **1982**, *104*, 1874.
(20) Dance, I. G. *J. Am. Chem. Soc.* **1980**, *102*, 3445.
(21) Kägi, J. H. R., Nordberg, M., Eds. "Metallothionein"; Birkhäuser Verlag: Basel, 1979.
(22) Kägi, J. H. R.; Vallee, B. L. *J. Biol. Chem.* **1961**, *236*, 2435. Kojima, Y.; Berger, C.; Vallee, B. L.; Kägi, J. H. R. *Proc. Natl. Acad. Sci. U.S.A.* **1976**, *73*, 3413.
(23) Two crab metallothioneins have recently been shown to contain 57 and 58 residues, both with 18 Cys residues: Lerch, K.; Ammer, D.; Olafson, R. W. *J. Biol. Chem.* **1982**, *257*, 2420.
(24) Otvos, J. D.; Armitage, I. M. *J. Am. Chem. Soc.* **1979**, *101*, 7734; *Proc. Natl. Acad. Sci. U.S.A.* **1980**, *77*, 7094.
(25) Otvos, J. D.; Olafson, R. W.; Armitage, I. M. *J. Biol. Chem.* **1982**, *257*, 2427.
(26) (a) Vašák, M. *J. Am. Chem. Soc.* **1980**, *102*, 3953. (b) Vašák, M.; Kägi, J. H. R.; Holmquist, B.; Vallee, B. L. *Biochemistry* **1981**, *20*, 6659. (c) Vašák, M.; Kägi, J. H. R. *Proc. Natl. Acad. Sci. U.S.A.* **1981**, *78*, 6709.

0020-1669/82/1321-3928$01.25/0

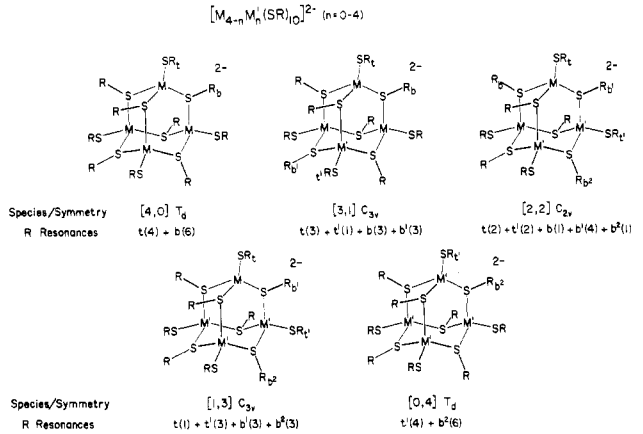

Figure 1. Schematic representation of the cage structures in the series $[M_{4-n}M'_n(SR)_{10}]^{2-}$. The type (b = bridging, t = terminal) and number of R groups under the idealized $[M_{4-n}M'_n(\mu\text{-}SR)_6]^{2+}$ core unit symmetries are given. Only one R group of a given type is labeled.

because of the cysteinate:metal ratio, must be bridged to one another. The presence of bridged sites is further indicated by the magnetic and EPR characteristics of the Co(II) proteins.[26c] The cage complexes $[M_4(SPh)_{10}]^{2-}$, with tetrahedral $M^{II}(SPh)(\mu\text{-}SPh)_3$ sites, are modest, symmetrized examples of the same general circumstance.

Recently we have been investigating certain reactions of biologically significant cluster and cage complexes. The ferredoxin site analogues $[Fe_2X_2(SR)_4]^{2-}$ and $[Fe_4X_4(SR)_4]^{2-,3-}$ have been shown to undergo X = S/Se exchange reactions with retention of overall structure.[27] The first demonstration of reactivity of $[M_4(SPh)_{10}]^{2-}$ cages has been afforded by quantitative formation of $[Fe_4S_4(SPh)_4]^{2-}$ from the M = Fe(II) complex in reactions with elemental sulfur.[15,28] More recently, $[Co_4(SPh)_{10}]^{2-}$ and HS^- have been shown to give the octanuclear cluster $[Co_8S_6(SPh)_8]^{4-}$ in 50% yield.[29] Here we describe another type of reaction of these complexes but one that leaves intact the cage structure, viz., facile metal ion exchange in the systems $[M_4(SPh)_{10}]^{2-}/[M'_4(SPh)_{10}]^{2-}$. Also included is the detailed structure of $[Fe_4(SPh)_{10}]^{2-}$, which had been briefly described earlier.[15]

Experimental Section

Preparation of Compounds. Tetramethyl- or tetraethylammonium salts of $[Fe_4(SPh)_{10}]^{2-}$[28] and $[Co_4(SPh)_{10}]^{2-}$[16] were prepared as previously described. The following preparations and manipulations were conducted under a pure dinitrogen atmosphere with use of degassed solvents.

$(Me_4N)_2[Zn_4(SPh)_{10}]$. A solution of 6.81 g (50 mmol) of $ZnCl_2$ in 50 mL of methanol was added to a solution of 125 mmol of sodium benzenethiolate (from 2.87 g of sodium and 14.2 g of benzenethiol) in 150 mL of methanol. After the solution was stirred for 10 min, sodium chloride was removed by filtration and a solution of 4.6 g (22 mmol) of tetraethylammonium bromide was added. The resultant precipitate became microcrystalline upon further stirring of the reaction mixture. The product was collected by filtration, washed with methanol, and dried in vacuo, affording 16.9 g (90%) of white solid. Pure material was obtained by one recrystallization from acetonitrile. Anal. Calcd for $C_{68}H_{74}N_2S_{10}Zn_4$: C, 54.40; H, 4.97; N, 1.87; S, 21.35; Zn, 17.42. Found: C, 54.35; H, 4.96; N, 1.85; S, 21.21; Zn, 17.20.

$(Et_4N)_2[Zn_4(SPh)_{10}]$. This compound was prepared in comparable yield by a procedure analogous to that for the Me_4N^+ salt. Anal. Calcd for $C_{76}H_{90}N_2S_{10}Zn_4$: C, 56.57; H, 5.62; N, 1.74. Found: C, 55.85; H, 5.59; N, 1.89. $(Et_3NH)_2[Zn_4(SPh)_{10}]$ has been synthesized by an electrochemical method.[17]

$(Et_4N)_2[Cd(SPh)_4]$. A solution of 5.71 g (25 mmol) of $CdCl_2 \cdot {}^5/_2H_2O$ in 50 mL of methanol and 10 mL of water was added to a solution of 125 mmol of sodium benzenethiolate (from 2.87 g of sodium and 14.2 g of benzenethiol) in 100 mL of methanol. After the solution was stirred for 30 min, sodium chloride was removed by filtration and the filtrate was added to 10.5 g (50 mmol) of solid tetraethylammonium bromide. The volume of the solution was reduced in vacuo until incipient crystallization; the solution was gently warmed and then cooled slowly to −25 °C. The white crystals were collected by filtration, washed with ethanol and ether, and dried in vacuo to give 13.8 g (68%) of product. Anal. Calcd for $C_{40}H_{60}CdN_2S_4$: C, 59.34; H, 7.47; Cd, 13.88; N, 3.46; S, 15.84. Found: C, 59.57; H, 7.54; Cd, 13.42; N, 3.46; S, 15.80. $(Ph_4P)_2[Cd(SPh)_4]$ has been reported.[6]

$(Et_4N)_2[Cd_4(SPh)_{10}]$. A solution of 9.13 g (40 mmol) of $CdCl_2 \cdot {}^5/_2H_2O$ in 100 mL of methanol and 10 mL of water was added dropwise to a solution of 10.1 g (100 mmol) of triethylamine and 11.4 g (100 mmol) of benzenethiol in 150 mL of methanol. A solution of 4.2 g (20 mmol) of tetraethylammonium bromide in 50 mL of methanol was added to the cloudy solution, resulting in the separation of a crystalline solid. Acetone (50 mL) and acetonitrile (10 mL) were added, and the mixture was warmed to 55 °C to give a nearly clear solution. This solution was cooled to −25 °C, causing separation of a white crystalline solid. This material was collected by filtration, washed with methanol and ether, and dried in vacuo; 10 g (55%) of product was obtained. Anal. Calcd for $C_{76}H_{90}Cd_4N_2S_{10}$: C, 50.66; H, 5.03; Cd, 24.95; N, 1.55; S, 17.79. Found: C, 50.42; H, 5.05; Cd, 24.83; N, 1.66; S, 17.89. Crystal data: monoclinic ($P2_1/c$, a = 13.846 (5) Å, b = 34.782 (6) Å, c = 21.528 (8) Å, β = 130.84 (2)°, V = 7844 (3) Å^3.

$(Et_4N)_2[M(SPh\text{-}2,4,6\text{-}d_3)_{10}]$. The method of Best and Wilson[30] was used to prepare the hydrochloride of aniline-2,4,6-d_3. Recrystallized aniline hydrochloride (90 g) was dissolved in 90 mL of D_2O (99.7 atom % D), and the solution was refluxed for 24 h. The solvent was removed and replaced with fresh D_2O, and the solution was refluxed for 24 h. This cycle was repeated four times. The aniline-d_3 hydrochloride was converted to the thiol by the standard procedure[31] of reaction of ethyl xanthate with diazotized amine, base hydrolysis, and neutralization with acid. The product was extracted from the reaction mixture with ether. After distillation benzenethiol-2,4,6-d_3 was obtained in 45% yield. Relative ^{1}H NMR signal intensities (ring H, 7.2 ppm; SH, 3.90 ppm (CD_3CN)) indicated >90% ring deuteration, which was sufficient for *m*-H signal identification in spectra of complexes. The compounds $(Et_4N)_2[M_4(SPh\text{-}d_3)_{10}]$ (M = Fe(II), Co(II), Zn(II)) were prepared by the preceding and published[16,28] methods.

Collection and Reduction of X-ray Data. Red-brown, air-sensitive crystals were grown by slow cooling of an acetonitrile/butyronitrile solution of $(Me_4N)_2[Fe_4(SPh)_{10}]$. A single crystal was lodged in a glass capillary and sealed under argon. Data were collected at ambient temperature on a Nicolet R3M four-circle automated diffractometer using graphite-monochromatized Mo Kα radiation. The orientation matrix and unit cell dimensions were calculated by least-squares treatment of 25 machine-centered reflections ($20° < 2\theta < 30°$). The machine and crystal parameters are summarized in Table I. Three check reflections, measured every 60 reflections, exhibited no decay over the duration of data collection. The data were processed with the program XTAPE of the SHELXTL program package (Nicolet XRD Corp., Cupertino, CA). No absorption correction was applied. The systematic absences $0k0$ ($k \neq 2n$) and $h0l$ ($h + l \neq 2n$) uniquely define the nonstandard space group $P2_1/n$.

Solution and Refinement of the Structure. All calculations were carried out with SHELXTL programs. Atomic scattering factors were taken from the tabulation of Cromer and Waber.[32] The direct-methods program MULTAN revealed the atomic positions of the Fe_4S_{10} portion. All remaining non-hydrogen atoms were located, and their positional parameters were refined by using difference Fourier maps and blocked cascade least-squares refinement. Isotropic refinement of all non-hydrogen atoms converged at R = 10.0%. At this point there remained three peaks of intensities greater than 1 e/Å^3. All non-hydrogen atoms of the cations and anions were refined with anisotropic thermal parameters. In the last stage of this refinement

(27) Reynolds, J. G.; Holm, R. H. *Inorg. Chem.* **1981**, *20*, 1873.
(28) Hagen, K. S.; Reynolds, J. G.; Holm, R. H. *J. Am. Chem. Soc.* **1981**, *103*, 4054.
(29) Christou, G.; Hagen, K. S.; Holm, R. H. *J. Am. Chem. Soc.* **1982**, *104*, 1744.
(30) Best, A. P.; Wilson, C. L. *J. Chem. Soc.* **1946**, 239.
(31) Leuckart, R. *J. Prakt. Chem.* **1890**, *41*, 179.
(32) Cromer, D. T.; Waber, J. T. "International Tables for X-Ray Crystallography"; Kynoch Press: Birmingham, England, 1974.

Table I. Summary of Crystal Data, Intensity Collection, and Structure Refinement for $(Me_4N)_2[Fe_4(SPh)_{10}]\cdot C_4H_7N$

quantity	data
formula (mol wt)	$C_{72}H_{81}Fe_4N_3S_{10}$ (1532.50)
a, Å	14.314 (3)
b, Å	24.038 (5)
c, Å	22.101 (3)
β, deg	96.06 (1)
cryst system	monoclinic
V, Å^3	7560 (2)
Z	4
d_{calcd}, g/cm^3	1.35
d_{obsd}, g/cm^3	1.33[a]
space group	$P2_1/n$
cryst dimens, mm	0.48 × 0.24 × 0.26
radiation	Mo K$\bar{\alpha}$ (λ = 0.71069 Å)
abs coeff, μ, cm^{-1}	10.6
scan speed, deg/min	2.0–29.3 ($\theta/2\theta$ scan)
scan range, deg	2.0 + ($2\theta_{K\alpha_2}$–$2\theta_{K\alpha_1}$)
bkgd:scan time ratio	0.50
data collected	$3° \leq 2\theta \leq 43°$; $+h, +k, \pm l$
no. of unique data ($I > 3\sigma(I)$)	5470
no. of variables	776
goodness of fit	1.18
R, %	4.1
R_w, %	4.4

[a] Measured in CCl_4/hexane by the neutral-buoyancy technique.

fixed contributions from hydrogen atoms with thermal parameters set at 1.2× that of the bonded carbon atoms were included. A final difference Fourier map revealed five peaks of intensities greater than 1 e/Å^3. These were assigned to a butyronitrile solvate molecule (NC(1)C(2)C(3)C(4)). Isotropic refinement afforded ∠NC(1)C(2) = 175°, ∠C(1)C(2)C(3) = 98°, ∠C(2)C(3)C(4) = 99°, C(1)–N = 1.28 Å, C(1)–C(2) = 1.74 Å, C(2)–C(3) = 1.36 Å, and C(3)–C(4) = 1.42 Å. Unique data used in the refinement and final R factors are given in Table I. The following results are tabulated: positional parameters (Table II) and interatomic distances and angles (Table III) of the anion; thermal parameters of the anion (Table S-I) and positional and thermal parameters of the cations and solvate molecule (Table S-II); calculated H atom coordinates (Table S-III); values of $10|F_o|$ and $10|F_c|$ (Table S-IV).[33]

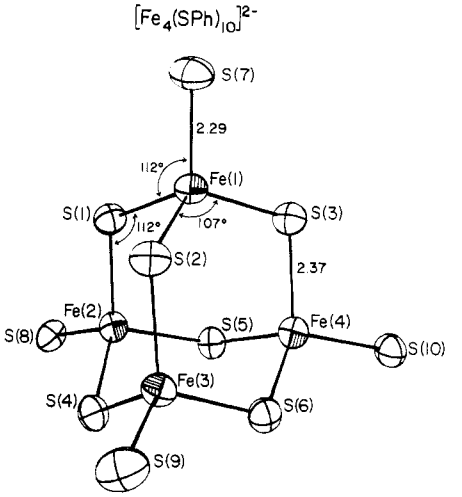

Figure 2. The structure of $[Fe_4(SPh)_{10}]^{2-}$ (phenyl groups omitted), showing 50% probability ellipsoids, the atom numbering scheme, and mean values of independent bond distances and angles under idealized T_d symmetry.

Table II. Positional Parameters of $[Fe_4(SPh)_{10}]^{2-}$

atom	x	y	z	atom	x	y	z
Fe(1)	0.36137 (6)[a]	0.32112 (3)	0.37804 (4)	C(1)S(5)	0.5758 (4)	0.2291 (3)	0.5460 (3)
Fe(2)	0.51276 (6)	0.18298 (3)	0.40069 (4)	C(2)S(5)	0.6689 (5)	0.2158 (3)	0.5400 (3)
Fe(3)	0.24561 (6)	0.17138 (3)	0.35208 (4)	C(3)S(5)	0.7403 (5)	0.2427 (4)	0.5758 (3)
Fe(4)	0.33477 (6)	0.22756 (4)	0.51724 (4)	C(4)S(5)	0.7216 (5)	0.2814 (3)	0.6176 (3)
S(1)	0.50473 (11)	0.27557 (7)	0.36172 (7)	C(5)S(5)	0.6287 (5)	0.2949 (3)	0.6229 (3)
S(2)	0.25706 (11)	0.26363 (7)	0.31540 (7)	C(6)S(5)	0.5574 (5)	0.2682 (3)	0.5883 (3)
S(3)	0.34727 (11)	0.32022 (7)	0.48349 (7)	C(1)S(6)	0.1156 (4)	0.1765 (2)	0.4708 (3)
S(4)	0.39115 (10)	0.12307 (7)	0.35743 (7)	C(2)S(6)	0.0574 (5)	0.2100 (3)	0.4340 (3)
S(5)	0.48409 (10)	0.18972 (7)	0.50393 (7)	C(3)S(6)	−0.0382 (5)	0.2116 (4)	0.4399 (4)
S(6)	0.23546 (10)	0.16722 (7)	0.45750 (7)	C(4)S(6)	−0.0736 (5)	0.1799 (4)	0.4828 (4)
S(7)	0.33766 (13)	0.40796 (7)	0.33730 (8)	C(5)S(6)	−0.0158 (5)	0.1462 (4)	0.5210 (3)
S(8)	0.66064 (11)	0.14780 (7)	0.39048 (7)	C(6)S(6)	0.0786 (4)	0.1450 (3)	0.5154 (3)
S(9)	0.12787 (12)	0.13181 (8)	0.28843 (8)	C(1)S(7)	0.4028 (5)	0.4612 (3)	0.3756 (3)
S(10)	0.29306 (12)	0.23405 (7)	0.61392 (7)	C(2)S(7)	0.4961 (6)	0.4568 (4)	0.3933 (4)
C(1)S(1)	0.5025 (4)	0.2696 (2)	0.2806 (3)	C(3)S(7)	0.5484 (9)	0.5005 (5)	0.4214 (5)
C(2)S(1)	0.4755 (5)	0.3148 (3)	0.2430 (3)	C(4)S(7)	0.5043 (12)	0.5483 (6)	0.4313 (6)
C(3)S(1)	0.4719 (5)	0.3092 (3)	0.1808 (3)	C(5)S(7)	0.4116 (11)	0.5547 (5)	0.4151 (5)
C(4)S(1)	0.4949 (5)	0.2607 (3)	0.1544 (3)	C(6)S(7)	0.3606 (7)	0.5111 (3)	0.3869 (4)
C(5)S(1)	0.5215 (5)	0.2166 (3)	0.1908 (3)	C(1)S(8)	0.6782 (4)	0.0831 (3)	0.4287 (3)
C(6)S(1)	0.5253 (5)	0.2207 (3)	0.2533 (3)	C(2)S(8)	0.6074 (4)	0.0515 (3)	0.4487 (3)
C(1)S(2)	0.1422 (4)	0.2936 (3)	0.3079 (3)	C(3)S(8)	0.6255 (5)	0.0014 (3)	0.4772 (3)
C(2)S(2)	0.1178 (4)	0.3342 (3)	0.3466 (3)	C(4)S(8)	0.7161 (6)	−0.0177 (3)	0.4880 (3)
C(3)S(2)	0.0301 (5)	0.3590 (4)	0.3373 (4)	C(5)S(8)	0.7869 (5)	0.0126 (3)	0.4685 (3)
C(4)S(2)	−0.0341 (5)	0.3423 (3)	0.2888 (4)	C(6)S(8)	0.7706 (5)	0.0628 (3)	0.4396 (3)
C(5)S(2)	−0.0089 (5)	0.3005 (3)	0.2504 (4)	C(1)S(9)	0.0844 (4)	0.0675 (3)	0.3125 (3)
C(6)S(2)	0.0775 (4)	0.2769 (3)	0.2601 (3)	C(2)S(9)	0.0588 (4)	0.0263 (3)	0.2705 (3)
C(1)S(3)	0.2454 (4)	0.3591 (3)	0.4969 (3)	C(3)S(9)	0.0155 (5)	−0.0214 (3)	0.2862 (4)
C(2)S(3)	0.2441 (6)	0.4159 (3)	0.4875 (3)	C(4)S(9)	−0.0036 (5)	−0.0294 (3)	0.3452 (4)
C(3)S(3)	0.1660 (8)	0.4464 (4)	0.4967 (5)	C(5)S(9)	0.0224 (5)	0.0096 (3)	0.3876 (3)
C(4)S(3)	0.0895 (8)	0.4210 (5)	0.5166 (5)	C(6)S(9)	0.0664 (4)	0.0572 (3)	0.3723 (3)
C(5)S(3)	0.0886 (6)	0.3645 (5)	0.5264 (4)	C(1)S(10)	0.2804 (4)	0.1686 (3)	0.6475 (3)
C(6)S(3)	0.1668 (5)	0.3336 (3)	0.5160 (3)	C(2)S(10)	0.2222 (5)	0.1645 (3)	0.6936 (3)
C(1)S(4)	0.4210 (4)	0.0978 (2)	0.2859 (3)	C(3)S(10)	0.2123 (6)	0.1141 (4)	0.7224 (4)
C(2)S(4)	0.5022 (4)	0.0661 (3)	0.2835 (3)	C(4)S(10)	0.2593 (6)	0.0680 (4)	0.7057 (4)
C(3)S(4)	0.5235 (5)	0.0430 (3)	0.2292 (3)	C(5)S(10)	0.3157 (6)	0.0717 (3)	0.6600 (4)
C(4)S(4)	0.4646 (5)	0.0504 (3)	0.1778 (3)	C(6)S(10)	0.3263 (5)	0.1215 (3)	0.6308 (3)
C(5)S(4)	0.3860 (6)	0.0818 (4)	0.1791 (3)				
C(6)S(4)	0.3631 (5)	0.1062 (3)	0.2326 (3)				

[a] Estimated standard deviations in the least significant figure(s) are given in this and subsequent tables.

Table III. Selected Interatomic Distances (Å) and Angles (Deg) for $(Me_4N)_2[Fe_4(SPh)_{10}]$

		Fe–S_t[a]	
Fe(1)–S(7)	2.284 (2)	Fe(4)–S(10)	2.284 (2)
Fe(2)–S(8)	2.313 (2)	mean	2.292 (14)[b]
Fe(3)–S(9)	2.285 (2)		
		Fe–S_b[a]	
Fe(1)–S(1)	2.387 (2)	Fe(3)–S(4)	2.377 (2)
Fe(1)–S(2)	2.370 (2)	Fe(3)–S(6)	2.352 (2)
Fe(1)–S(3)	2.360 (2)	Fe(4)–S(3)	2.362 (2)
Fe(2)–S(1)	2.385 (2)	Fe(4)–S(5)	2.369 (2)
Fe(2)–S(4)	2.380 (2)	Fe(4)–S(6)	2.339 (2)
Fe(2)–S(5)	2.366 (2)	mean	2.368 (14)
Fe(3)–S(2)	2.373 (2)		
		Fe···Fe	
Fe(1)–Fe(2)	3.968 (2)	Fe(2)–Fe(4)	3.957 (2)
Fe(1)–Fe(3)	3.979 (2)	Fe(3)–Fe(4)	3.974 (2)
Fe(1)–Fe(4)	3.862 (2)	mean	3.935 (54)
Fe(2)–Fe(3)	3.871 (2)		
		S_b···S_b	
S(1)–S(2)	3.595 (2)	S(3)–S(5)	3.699 (3)
S(1)–S(3)	3.841 (3)	S(3)–S(6)	4.028 (3)
S(1)–S(4)	4.007 (3)	S(4)–S(5)	3.728 (2)
S(1)–S(5)	3.797 (3)	S(4)–S(6)	3.467 (3)
S(2)–S(3)	4.038 (3)	S(5)–S(6)	3.638 (2)
S(2)–S(4)	3.948 (3)	mean	3.81 (19)
S(2)–S(6)	3.941 (3)		
		C–C	
range	1.340 (20)–1.406 (9)	mean	1.375 (14)
		S–C	
range	1.748 (7)–1.796 (6)	mean	1.778 (16)
		N–C (Me_4N^+)	
range	1.36 (2)–1.48 (1)	mean	1.44 (4)
		S_b–Fe–S_t	
S(1)–Fe(1)–S(7)	117.0 (1)	S(4)–Fe(3)–S(9)	114.4 (1)
S(2)–Fe(1)–S(7)	104.1 (1)	S(6)–Fe(3)–S(9)	118.3 (1)
S(3)–Fe(1)–S(7)	111.9 (1)	S(3)–Fe(4)–S(10)	105.5 (1)
S(1)–Fe(2)–S(8)	108.4 (1)	S(5)–Fe(4)–S(10)	118.1 (1)
S(4)–Fe(2)–S(8)	112.2 (1)	S(6)–Fe(4)–S(10)	111.5 (1)
S(5)–Fe(2)–S(8)	111.9 (1)	mean	111.5
S(2)–Fe(3)–S(9)	104.6 (1)		
		S_b–Fe–S_b	
S(1)–Fe(1)–S(2)	98.2 (1)	S(2)–Fe(3)–S(6)	113.1 (1)
S(1)–Fe(1)–S(3)	108.0 (1)	S(4)–Fe(3)–S(6)	94.3 (1)
S(2)–Fe(1)–S(3)	117.2 (1)	S(3)–Fe(4)–S(5)	102.9 (1)
S(1)–Fe(2)–S(4)	114.5 (1)	S(3)–Fe(4)–S(6)	117.9 (1)
S(1)–Fe(2)–S(5)	106.1 (1)	S(5)–Fe(4)–S(6)	101.2 (1)
S(4)–Fe(2)–S(5)	103.6 (1)	mean	107.4
S(2)–Fe(3)–S(4)	112.4 (1)		
		Fe–S_b–Fe	
Fe(1)–S(1)–Fe(2)	112.5 (1)	Fe(2)–S(5)–Fe(4)	113.4 (1)
Fe(1)–S(2)–Fe(3)	114.0 (1)	Fe(3)–S(6)–Fe(4)	115.8 (1)
Fe(1)–S(3)–Fe(4)	109.7 (1)	mean	112.4
Fe(2)–S(4)–Fe(3)	108.9 (1)		

[a] t = terminal, b = bridging ligand. [b] The standard deviation of the mean was estimated from $\sigma \approx s = [(\Sigma x_i^2 - n\bar{x}^2)/(n-1)]^{1/2}$.

Other Physical Measurements. All samples were prepared and measured under anaerobic conditions. Absorption spectra were obtained with a Cary Model 17 or 219 spectrophotometer. NMR spectra were recorded on a Bruker WM-300 spectrometer equipped with a deuterium lock and a temperature controller. ^1H spectra were measured at 300 MHz with Me_4Si internal reference; shifts downfield and upfield of the reference are designated as negative and positive, respectively. ^{113}Cd spectra (natural-abundance samples, 12.3% ^{113}Cd) were measured at 66.58 MHz. For consistency with earlier work[34] shifts were externally referenced to an aqueous 0.1 M $Cd(ClO_4)_2$ solution. Solutions used to investigate M/M′ exchange reactions by ^1H NMR were prepared by mixing aliquots of standard CD_3CN solutions prepared by weight from isolated salts of $[M_4(SPh)_{10}]^{2-}$. Final solutions were 20–800 mM in total metal. In all cases equilibrium was rapidly established upon mixing; all observations refer to equilibrium systems.

Table IV. Comparative Structural Features of Cage Complexes

compd	dist, Å		vol, Å^3	
	M···M	S_b···S_b	M_4	S_6
$(Me_4N)_2[Co_4(SPh)_{10}]^a$	3.87 (2)	3.74 (14)	6.83	24.62
$(Me_4N)_2[Fe_4(SPh)_{10}]^b$	3.94 (5)	3.81 (19)	7.18	26.09
$(Ph_4P)_2[Fe_4(SPh)_6Cl_4]^c$	3.94 (4)	3.79 (18)	7.21	25.72
$(Me_4N)_2[Zn_4(SPh)_8Cl_2]^d$	3.90 (5)	3.81 (12)	7.00	26.13

[a] Reference 16. [b] This work. [c] Reference 19. [d] Reference 18.

Results and Discussion

Description of the Structure of $[Fe_4(SPh)_{10}]^{2-}$. The crystal structure of $(Me_4N)_2[Fe_4(SPh)_{10}]$, obtained as a butyronitrile monosolvate, contains well-separated anions, cations, and solvate molecules. The structure of the Fe_4S_{10} portion of the anion is presented in Figure 2, a stereoview of the entire anion is provided in Figure 3, and selected interatomic distances and angles are compiled in Table III. The adamantane-like stereochemistry of the $Fe_4(\mu\text{-}S)_6$ cage, composed of a nearly regular Fe_4 tetrahedron and a distorted S_6 octahedron, is immediately evident. Because $M_4(\mu\text{-}S)_6$ structures of this type have been described in some detail earlier,[16,18-20] the leading structural features of $[Fe_4(SPh)_{10}]^{2-}$ are briefly summarized. (i) There is no crystallographically imposed symmetry, nor does the $Fe_4(\mu\text{-}S)_6$ cage closely approach the T_d symmetry of adamantane. (ii) Deviations from idealized T_d skeletal symmetry are evident in all metrical features involving bridging (b) atoms and are most obvious from the large ranges of S_b–Fe–S_b angles (94.3 (1)–117.9 (1)°) and nonbonded S_b···S_b distances (3.467 (3)–4.038 (3) Å). (iii) Coordination of each Fe atom is completed by one terminal (t) benzenethiolate ligand, with appreciable departures from idealized C_{3v} site symmetry indicated by the variation (104.6 (1)–118.3 (1)°) in S_b–Fe–S_t angles. (iv) The mean value of Fe–S_b distances exceeds that of Fe–S_t distances by ~0.08 Å. The latter value (2.29 (1) Å) is somewhat smaller than the mean Fe–S distance (2.353 (9) Å) in $[Fe(SPh)_4]^{2-}$,[7] a circumstance presumably due to the necessarily smaller contribution of bridging vs. terminal ligands in approaching electroneutrality within FeS_4 coordination units. (v) Fe···Fe distances (mean value 3.94 (5) Å) are too long for direct metal–metal interactions. (vi) The six axial phenyl groups in the four chair Fe_3S_3 rings of the cage occur in the 3–2–1–0 pattern (Figure 3), specified by the number of axial groups in each ring.

Structural comparison of $[Fe_4(SPh)_{10}]^{2-}$ with other $M_4(\mu\text{-}SPh)_6$ cage complexes is hindered to an extent by differing distortions of the cages from idealized T_d symmetry, in which all distances and angles are equal. This situation leads to large esd values of mean distances and wide variations in cage internal angles and arises in part from different axial group patterns in individual $Fe_3(\mu\text{-}SPh)_3$ rings. Whereas the 3–2–1–0 arrangement of $[Fe_4(SPh)_{10}]^{2-}$ is retained in $(Ph_4P)_2[Fe_4(SPh)_6Cl_4]$,[19] the remaining complexes in Table IV have the 2–2–1–1 arrangement. The angles S_{ax}–M–S_{ax} are invariably larger than S_{ax}–M–S_{eq} and S_{eq}–M–S_{eq} angles in a given ring. The third possible axial group pattern, 3–1–1–1, has not yet been observed. As an alternative to distance and angle comparisons the structures of discrete cage complexes are compared in Table IV in terms of the volumes of their (imperfect) M_4 tetrahedra and S_6 octahedra calculated from atomic coordinates. In order of listing in the table these stand in the ratios 1:1.05:1.06:1.02 and 1:1.06:1.04:1.06, respectively. Taking the mean Co···Co and Co–S_b (2.32 Å) distances in $[Co_4(SPh)_{10}]^{2-}$[16] as bases, correcting corresponding M =

(33) See paragraph at end of this article regarding supplementary material.
(34) Haberkorn, R. A.; Que, L., Jr.; Gillum, W. O.; Holm, R. H.; Liu, C. S.; Lord, R. C. *Inorg. Chem.* **1976**, *15*, 2408.

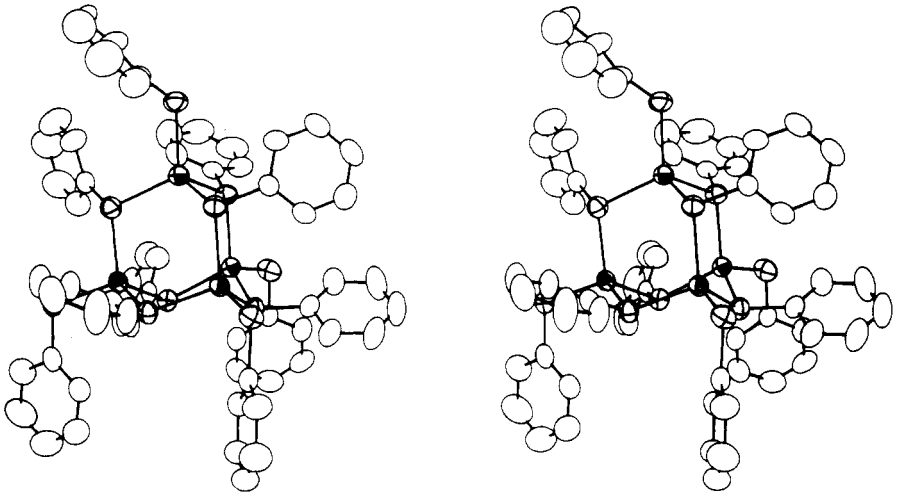

Figure 3. Stereoview of the structure of $[Fe_4(SPh)_{10}]^{2-}$, with 50% probability ellipsoids of Fe and S atoms depicted.

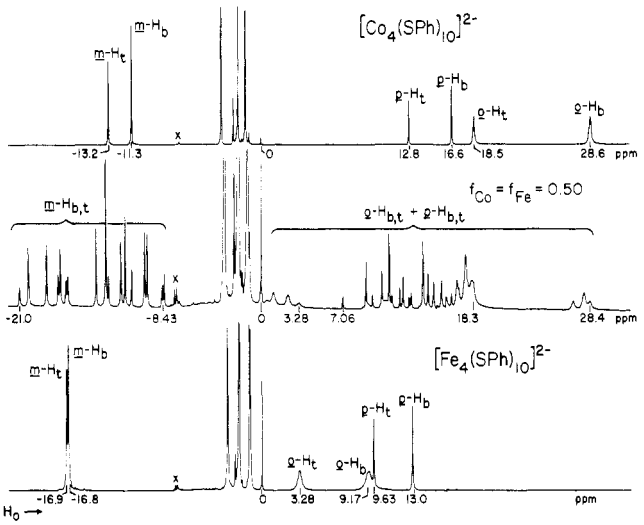

Figure 4. ^1H NMR spectra (300 MHz) of $[Co_4(SPh)_{10}]^{2-}$, $[Fe_4(SPh)_{10}]^{2-}$, and a 1:1 mixture of these complexes in CD_3CN solutions at 238 K (× = impurity).

Fe(II), Zn(II) distances to them using Shannon tetrahedral radii,[35] and assuming T_d cage symmetry, we find the volume ratios for M = Co(II)/Fe(II)/Zn(II) structures are 1:1.08:1.03 (M_4) and 1:1.06:1.02 (S_6). Thus the observed volumes of these units increase in the order of M(II) radii, with the exception of $[Zn_4(SPh)_8Cl_2]^{2-}$, whose S_6 octahedron is slightly larger than expected on this basis.[36] Relative volumes provide a simple index of metrical changes in $M_4(\mu\text{-}S)_6$ cages. Further, their small differences in real (≤6%) and idealized (≤8%) structures enhance the possibility of mixed-metal cage formation, at least with M = Fe(II), Co(II), and Zn(II), a matter confirmed in this work (vide infra).

Stereochemical Nonrigidity of $[M_4(SPh)_{10}]^{2-}$. The ^1H NMR spectra of paramagnetic $[Co_4(SPh)_{10}]^{2-}$ and $[Fe_4(SPh)_{10}]^{2-}$ at 238 K, shown in Figure 4, reveal isotropically shifted resonances whose line widths and relative intensities lead to the assignments indicated. These were confirmed by the spectra of the $[M_4(SPh\text{-}d_3)_{10}]^{2-}$ species, which gave only the downfield pair of signals in each case. Further, the spectrum of $[Fe_4(S\text{-}p\text{-}C_6H_4Me)_{10}]^{2-}$ (at 268 K[28]) lacks the sharp pair of upfield signals assigned to $p\text{-}H_{t,b}$. Spectra of these and the analogous Zn(II) and Cd(II) complexes when recorded at higher temperatures reveal the occurrence of an exchange process. Selected spectra are presented in Figure 5. The $m\text{-}H_t$ and $m\text{-}H_b$ resonances of $[Fe_4(SPh)_{10}]^{2-}$, partially resolved in the slow-exchange region at 239 K, coalesce at 305 K, and the averaged signal sharpens at higher temperatures. The same coalescence temperature was observed in 5 and 50 mM solutions, indicating that the process is intramolecular. In the case of $[Co_4(SPh)_{10}]^{2-}$ complete averaging was not observed at the highest temperature of measurement (346 K) but the onset of $m\text{-}H_t/m\text{-}H_b$ coalescence is evident. The spectrum of $[Zn_4(SPh)_{10}]^{2-}$ at slow exchange (239 K) is assigned as shown from relative signal intensities and the spectrum of $[Zn_4(SPh\text{-}d_3)_{10}]^{2-}$, whose $m\text{-}H_b$ and $m\text{-}H_t$ resonances occur at −6.91 and −6.88 ppm, respectively. Spectra at higher temperatures (not shown) reveal exchange averaging of the o-H doublets (−7.42, −7.15 ppm) and merging of the −7.02-ppm doublet with the multiplet centered at ∼−6.9 ppm. Coalescence occurs at 322 K. The spectrum at 346 K consists of an o-H signal and a composite m-H + p-H signal, whose intensity ratio is 2:3. The averaged spectrum of $[Zn_4(SPh\text{-}d_3)_{10}]^{2-}$ consists of one signal at −6.87 ppm, confirming the assignments given. With $[Cd_4(SPh)_{10}]^{2-}$ the spectrum at the lowest temperature of measurement (239 K) reveals exchange averaging. The fast-exchange regime is reached at higher temperatures, with a 2:3 intensity ratio of the o-H doublet and the m-H + p-H multiplet found in the 322 K spectrum. The similarity of spectra of $[Zn_4(SPh)_{10}]^{2-}$ and $[Cd_4(SPh)_{10}]^{2-}$, near or at the fast-exchange limit, provides reasonable evidence that the latter complex also possesses adamantane-like stereochemistry. Its structure has not yet been established by X-ray diffraction.

The observed stereochemical nonrigidity of the $[M_4(SPh)_{10}]^{2-}$ cages results in equilibration of bridging and terminal ligands. A plausible description of the process is offered in Figure 6. Two skeletal M–S bonds are ruptured followed by the onset of rotation about an intact M–S bond (I). Further rotation places an original terminal ligand SR* near a bridging position and shifts two initially bridging ligands near a bridging and a terminal position (II). M–S bond formation involving the three rotated ligands recovers the cage structure with the resultant change $SR^*_t \rightarrow SR^*_b$ (III). Repetitions of this process will lead to further degenerate SR_b exchange and $SR_t \rightleftharpoons SR_b$ scrambling. Although rate constants were not determined it is obvious that $k(Cd) >> k(Zn)$. This is consistent with quantitative kinetics of inversion of tetrahedral Zn(II) and Cd(II) complexes[37] and with the general trend of in-

(35) Co(II), 0.72 Å; Fe(II), 0.77 Å; Zn(II), 0.74 Å: R. D. Shannon, *Acta Crystallogr., Sect. A* **1976**, *A32*, 751.

(36) Insufficient crystallographic data were presented for $(Et_3NH)_2[Zn_4(SPh)_{10}]$[17] to allow meaningful volume calculation.

(37) Eaton, S. S.; Holm, R. H. *Inorg. Chem.* **1971**, *10*, 1446.

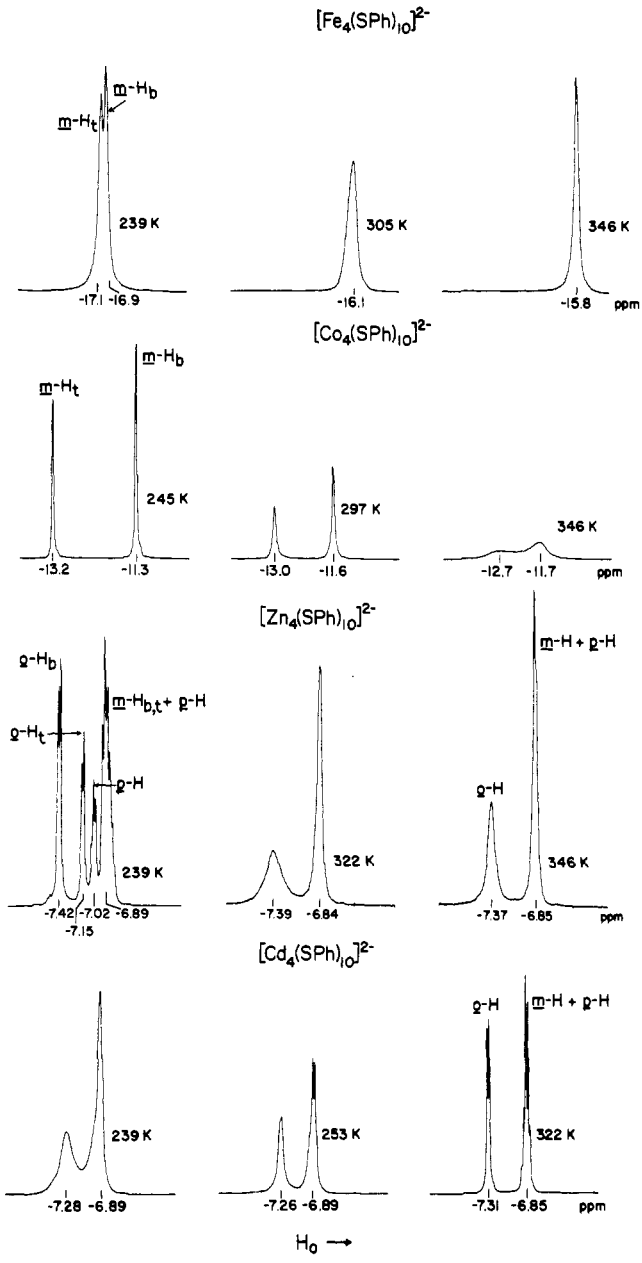

Figure 5. Temperature dependencies of the ^1H NMR spectra (300 MHz) of $[Fe_4(SPh)_{10}]^{2-}$ (50 mM, *m*-H), $[Co_4(SPh)_{10}]^{2-}$ (20 mM, *m*-H), and $[M_4(SPh)_{10}]^{2-}$ (M = Zn(II), Cd(II); 20 mM, phenyl H) in CD_3CN solutions. Each set of spectra is normalized to constant intensity vs. the $(CH_3CH_2)_4N^+$ resonance (not shown).

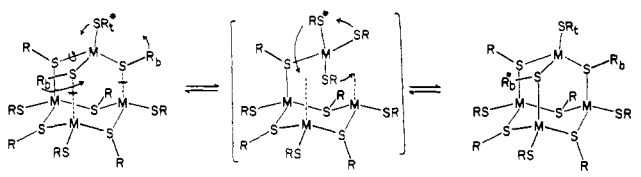

Figure 6. Mechanistic scheme for the stereochemical nonrigidity of $[M_4(SPh)_{10}]^{2-}$ cages resulting in the interconversion $SR_b \rightleftharpoons SR_t$ of bridging and terminal ligands.

creasing intramolecular rearrangement rates of $d^{0,10}$ complexes with increasing size of the metal ion[38] (Cd(II), 0.92 Å[35]).

(38) Holm, R. H. In "Dynamic Nuclear Magnetic Resonance Spectroscopy"; Jackman, L. M., Cotton, F. A., Eds.; Academic Press: New York, 1975; Chapter 9.

(39) Calingaert, G.; Beatty, H. A. *J. Am. Chem. Soc.* **1939**, *61*, 2748. Pinnavaia, T. J.; Fay, R. C. *Inorg. Chem.* **1966**, *5*, 233.

Table V. Equilibrium Constants for Metal Ion Exchange Reactions in $[M_4(SPh)_{10}]^{2-}/[M'_4(SPh)_{10}]^{2-}$ Systems in CD_3CN Solutions at ~240 K

M/M'	K_2	K_3	K_4
Fe(II)/Co(II)	2.0[a]	2.4 (1)[b]	2.6[a]
Co(II)/Zn(II)	2.2 (2)	2.4 (4)	2.5 (3)
Co(II)/Cd(II)	2.9 (3)	2.5 (3)	*c*
statistical	2.67	2.25	2.67

[a] Mean of two determinations. [b] Standard deviation given for the mean of three to five determinations. [c] Not determined.

Metal Ion Exchange Reactions. Exchange of metal ions among cage complexes may be represented by the process (1),

$$\underset{[4,0]}{[M_4(SPh)_{10}]^{2-}} + \underset{[0,4]}{[M'_4(SPh)_{10}]^{2-}} \rightleftharpoons \sum_{n=1}^{3} \underset{[4-n,\,n]}{[M_{4-n}M'_n(SPh)_{10}]^{2-}} \quad (1)$$

which includes the designations used hereafter for unmixed- and mixed-metal species. The reaction system involves five species and six equilibria with three independent equilibrium quotients that here have been chosen as those for reactions 2–4. Equilibrium systems of this general type have been

$$[4,0] + [2,2] \overset{K_2}{\rightleftharpoons} 2[3,1] \quad (2)$$

$$[3,1] + [1,3] \overset{K_3}{\rightleftharpoons} 2[2,2] \quad (3)$$

$$[2,2] + [0,4] \overset{K_4}{\rightleftharpoons} 2[1,3] \quad (4)$$

treated previously;[27,39] statistical values of the equilibrium constants are given in Table V. The symmetries and types and numbers of bridging and terminal ligands under these symmetries for the five possible complexes present in an equilibrium mixture are provided in Figure 1. These symmetries are idealized in that each

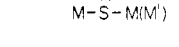

fragment is assumed to have effective C_s local symmetry; i.e., pyramidal inversion at S_b atoms is fast on the NMR time scale. Justification of this assumption is provided in Figure 4. Spectra of $[Co_4(SPh)_{10}]^{2-}$ and $[Fe_4(SPh)_{10}]^{2-}$, recorded in the slow-exchange limit of the $SR_b \rightleftharpoons SR_t$ process, are consistent with T_d symmetry rather than with the presence of frozen 3–2–1–0 and 2–2–1–1 conformational arrangements, respectively. In these arrangements all the ligands are inequivalent.

1. $[Fe_{4-n}Co_n(SPh)_{10}]^{2-}$ (M = Fe, M' = Co). Metal ion exchange was first observed in this system. The complete spectrum at 238 K of a system with equal mole fractions (*f*) of initial complexes is shown in Figure 4. Resonances extend over a 49-ppm range. The 17 *m*-H resonances of a mixture of five species, all at slow exchange with respect to $SR_b \rightleftharpoons SR_t$ interconversion and intermolecular metal ion exchange, are observed. Some 27 of the 34 *o*-H + *p*-H signals are partially resolved or fully resolved. The excellent resolution, especially in the *m*-H region (13-ppm range), is a consequence of isotropic interactions, which magnify intrinsic chemical shift differences. Sign alteration of *o*-, *m*-, and *p*-H isotropic shifts suggests that the dominant isotropic interaction is contact in origin. This is the usual case for tetrahedral Fe(II), but substantial dipolar shifts are a well-documented property of tetrahedral Co(II).[40] In this and other systems signals as-

(40) Horrocks, W. D. In "NMR of Paramagnetic Molecules"; La Mar, G. N., Horrocks, W. D., Holm, R. H., Eds.; Academic Press: New York, 1973; Chapter 4.

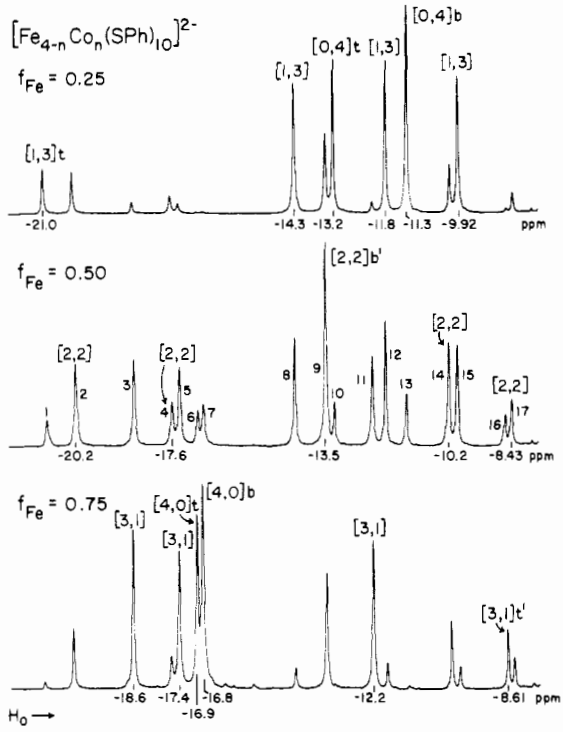

Figure 7. ^{1}H NMR spectra (300 MHz, *m*-H) of the system $[Fe_{4-n}Co_n(SPh)_{10}]^{2-}$ at the mole fractions f_{Fe} = 0.25, 0.50, and 0.75 in CD_3CN solutions at 238 K. Signal assignments are given in the notation of Figure 1.

signed as *m*-H were confirmed by spectra of $[M_4(SPh\text{-}d_3)_{10}]^{2-}$ complexes, only *m*-H resonances are utilized because of their better resolution, and spectra were recorded at ~240–250 K to suppress exchange processes and otherwise improve resolution. Equilibrium constants evaluated from integrated signal intensities are collected in Table V.

Spectra of solutions with different mole fractions f_{Fe} are contained in Figure 7. Peaks due to [4,0] and [0,4] species are readily identified from Figure 4. Those arising from mixed $[4-n, n]$ complexes in this and subsequent systems were assigned from intensity changes as dependent on f_M, with the assumption of roughly statistical exchange, and from relative intensities at fixed f_M. In this way all 17 *m*-H resonances have been unambiguously assigned as shown to individual species, but assignment of all resonances of a given species to specific inequivalent ligands (Figure 1) is not possible in this system. Thus for [3,1] and [1,3], each of which has four resonances, only the intensity-determined signals of t^1 and t, respectively, can be assigned. Similarly, of the five [2,2] resonances b^1 can be assigned and signals 4 + 17 and 2 + 14 are unequivocally related to b + b^2 and t + t^1, respectively. No definite assignments of members of pairs of signals can be made. This problem arises because neither the contact nor dipolar shift effected by a given M(II) or M(II)′ is constant from one species to another. As shown for $[Co_4(SPh)_{10}]^{2-}$ metal spins are weakly coupled;[16] modulation of such coupling affects contact shifts.[41] Dipolar shifts are sensitive to magnetic anisotropy and nuclear positions relative to local magnetic axes,[40] properties which will vary in the series $[4-n, n]$.

2. $[Co_{4-n}Zn_n(SPh)_{10}]^{2-}$ (M = Co, M′ = Zn). Occurrence of metal ion exchange is demonstrated by the spectra at different f_{Co} values presented in Figure 8. Spectra of species containing the SPh-d_3 ligand are shown in order to avoid difficulties with *o*-H and/or *p*-H signals in the −7 to −10 ppm

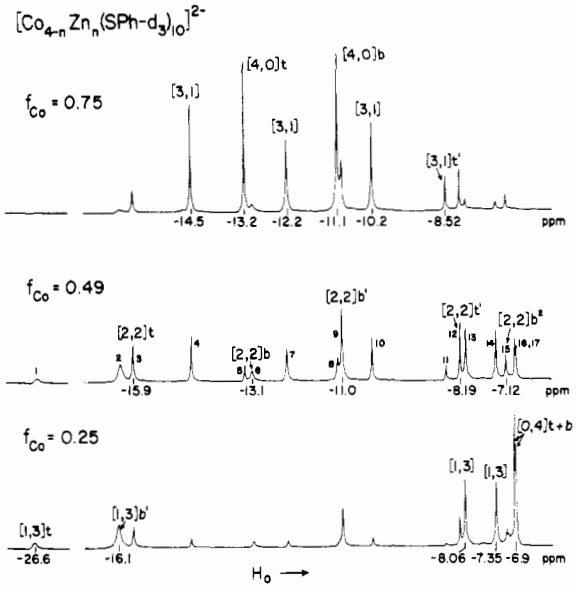

Figure 8. ^{1}H NMR spectra (300 MHz, *m*-H) of the system $[Co_{4-n}Zn_n(SPh\text{-}d_3)_{10}]^{2-}$ at the mole fractions f_{Co} = 0.25, 0.49, and 0.75 in CD_3CN solutions at 238 K. Spectra are normalized as in Figure 5, and signal assignments are given as in Figure 7.

range. Seventeen *m*-H signals over a 20-ppm range are resolved; the two resonances of the diamagnetic [0,4] complex occur at highest field. Because of this effect assignments of [1,3] and [3,1] spectra that are somewhat more specific than possible for the preceding system can be made. These are included in Figure 8 with assignments uniquely defined by relative intensities. The strongly isotropically shifted signal 2 (−16.1 ppm) of [1,3] is assigned to b^1, in the bridging Co–S(Ph)–Zn units. The other two signals of [1,3] with intensity 3 (13, 14) cannot be distinguished, but they occur at higher field for both must arise from ligands (t^1 + b^1) bound only to Zn(II). In the [2,2] spectrum signal 15 (−7.12 ppm) is assigned to b^2 (bridging Zn–S(Ph)–Zn) and signal 12 (−8.19 ppm) to t^1 (Zn–SPh) on the basis of their high-field positions. The remaining [2,2] signals of intensities equal to those of signals 15 and 12, viz., 6 and 3, respectively, are assigned as indicated to ligands coordinated only to Co(II). The largest shifts of bridging and terminal ligands bound to Co(II) are found, as might be expected, in the [1,3] species, where Co(II) is magnetically dilute. Their positions may be compared to the *m*-H shift of tetrahedral $[Co(SPh)_4]^{2-}$, −18.6 ppm (CD_3CN, 238 K).

3. $[Co_{4-n}Cd_n(SPh)_{10}]^{2-}$ (M = Co, M′ = Cd). This system was examined at mole fractions f_{Co} = 0.25, 0.50, and 0.75. Spectra (not shown) are similar to those of the $[Co_{4-n}Zn_n(SPh)_{10}]^{2-}$ system. Ten signals are found at −10 to −27 ppm and are due to all species except [0,4]. Chemical shifts are within 0.5 ppm of those of corresponding Co/Zn species.

4. $[Fe_{4-n}Zn_n(SPh)_{10}]^{2-}$ (M = Fe, M′ = Zn). The spectrum in Figure 9 of a system at f_{Fe} = 0.50 prepared with the SPh-d_3 ligand reveals an equilibrium mixture of all five species. Ten *m*-H signals are observed in the −13 to −37 ppm interval; these must arise from ligands bound to at least one Fe(II) atom. The signal assignments given follow from intensity considerations with one exception. Noting the isotropic shift order t > b^1 for [2,2] and [1,3], we attribute the least shifted resonance (10, −13.1 ppm) of the three equally intense resonances of [3,1] to b^1, in the Fe–S(Ph)–Zn bridges. This assignment affords the bridge Fe–S(Ph)–Fe isotropic shift order [2,2]b > [3,1]b > [4,0]b and the terminal Fe–SPh isotropic shift order [1,3]t > [2,2]t > [3,1]t > [4,0]t. This is the expected order of magnetic dilution of Fe(II) sites and thus is consistent with dominant contact shifts, which at fixed temperature are pro-

(41) La Mar, G. N.; Eaton, G. R.; Holm, R. H.; Walker, F. A. *J. Am. Chem. Soc.* **1973**, *95*, 63.

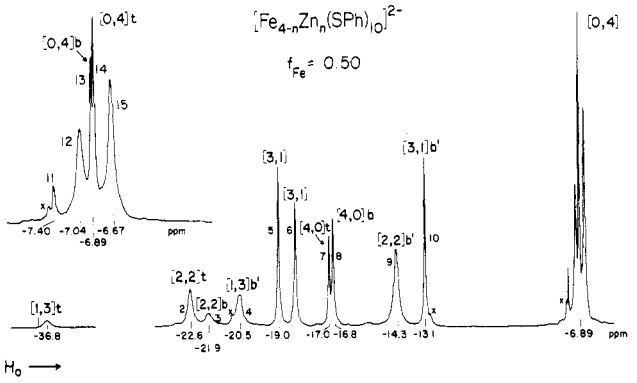

Figure 9. ^{1}H NMR spectra (300 MHz, *m*-H) of the system $[Fe_{4-n}Zn_n(SPh\text{-}d_3)_{10}]^{2-}$ at the mole fraction $f_{Fe} = 0.50$ in CD_3CN solution at ~250 K. Signal assignments are given as in Figure 7 (× = impurity).

portional to mean χ_{Fe} values.[41] The *m*-H shift of tetrahedral $[Fe(SPh)_4]^{2-}$ is −26.4 ppm (CD_3CN, 238 K). The shift order [1,3]t > [2,2]t > [4,0]t is observed in the $[Co_{4-n}Zn_n(SPh)_{10}]^{2-}$ system (Figure 8).

The $[Fe_{4-n}Cd_n(SPh)_{10}]^{2-}$ system at $f_{Fe} = 0.50$ was also examined. The spectrum in the *m*-H region (not shown) is very similar to that in Figure 9, demonstrating the occurrence of metal ion exchange and an equilibrium mixture of five species.

5. $[Zn_{4-n}Cd_n(SPh)_{10}]^{2-}$ (M = Zn, M′ = Cd). This system was investigated by natural-abundance ^{113}Cd NMR spectroscopy with 0.1 M total metal concentration in acetonitrile solutions at 291 K. The spectrum of $[Cd_4(SPh)_{10}]^{2-}$ consists of a single sharp resonance ($\Delta\nu_{1/2}$ 25 Hz) at 576.0 ppm downfield of the reference signal. In the range $0 < f_{Zn} \leq 0.6$ at least two additional signals are found within ±0.5 ppm of the [0,4] feature. None is due to $[Cd(SPh)_4]^{2-}$, whose signal occurs at 589.1 ppm. These results augment the original observation[34] that ^{113}Cd shifts of $Cd(SR)_4$ units (here with terminal or bridging and terminal ligands) occur downfield of 500 ppm. Resonances of the inequivalent Cd sites in metallothionein are somewhat more deshielded (600–670 ppm[24,25,42]). Recent measurements of Cd thiolate complexes generated in solution[43] indicate that shifts of R = alkyl vs. aryl species tend to occur at lower field, but none of these species (except $[Cd(SPh)_4]^{2-}$, tetrahedral in the solid state[6]) has been structurally characterized. The multiple signals observed in the present system suggest the occurrence of metal ion exchange but were insufficiently resolved for accurate integration. Although their chemical shift separations are comparable to ^{113}Cd–^{113}Cd coupling constants in metallothionein,[24,25] all [4 − *n*, *n*] species are expected to contain equivalent Cd sites (excluding isotope distribution effects). Further clarification of the system will require ^{113}Cd-enriched samples and measurements at lower temperatures.

In support of the foregoing interpretation of metal ion exchange with retention of cage structure, several observations are emphasized. (i) The 17 *m*-H signals required for an equilibrium mixture of the five species [4 − *n*, *n*] (*n* = 0–4) are observed in the Fe/Co system. (ii) The 10 *m*-H signals of the four species [4 − *n*, *n*] (*n* = 0–3) expected to be isotropically shifted as a consequence of binding to one or two paramagnetic metal ions are observed in the Co/Zn, Co/Cd, Fe/Zn, and Fe/Cd systems. (iii) No signals of significant intensity that are not assignable to [4 − *n*, *n*] species are observed. In particular, resonances of $[M(SPh)_4]^{2-}$ (M = Fe(II), Co(II)), conceivable cage degradation products, are absent.[44] (iv) Ligand field spectra of systems containing Fe(II) and Co(II) in acetonitrile solutions are consistent with the presence of tetrahedral M^{II}–S_4 chromophores only.[45] In the Fe/Zn system the Fe(II) $^5E \rightarrow {}^5T_2$ transition is shifted from 1850 to 1800 nm as $f_{Fe} = 1 \rightarrow 0.25$. Intensities at λ_{max} vary by <1% from those calculated on the basis of a simple dilution effect. In the Co/Zn and Co/Cd systems with $1 \geq f_{Co} \geq 0.25$ the Co(II) $\nu_2[^4A_2 \rightarrow {}^4T_1(F)]$ features at 1280 nm (sh, ~1400 nm) do not shift and their intensities are within 7% of those expected by dilution. In these and the Fe/Co system components of $\nu_3[^4A_2 \rightarrow {}^4T_2]$ do shift somewhat upon dilution[46] but no new features suggestive of a different type of chromophore appear. Band shifts are, therefore, a reflection of small changes in Co(II) sites as other M(II) atoms are incorporated in the cages.

Although not highly precise, the equilibrium constants for three systems (Table V) serve to demonstrate a roughly statistical distribution of products from reaction 1. This situation obtains with Cd(II)-containing cages despite the substantially larger radius of this ion.[47] Reaction 1 is the first well-documented case of metal ion exchange in small molecular cages. Some rough parallels are found in main-group cage chemistry, a recent example being the P_4S_3/As_4S_3 system.[48] Here the species $P_{4-n}As_nS_3$ (*n* = 1–3) have been detected by ^{31}P NMR spectroscopy; atom exchange was accomplished by fusion of the initial components. The exchange reactions demonstrated in this work are spontaneous. Their rapid occurrence is presumably a consequence of intramolecular lability. Reaction between cages with weakened or broken skeletal bonds (I and II in Figure 6) represents one conceivable pathway for metal ion exchange.

Attention has also been drawn by others[16,26b,c] to a possible relationship between adamantane-like $M_4(SR)_{10}$ cages and M(II) binding sites in metallothionein. Proposed models for tri- and tetranuclear aggregates, from ^{113}Cd NMR results with rabbit liver and crab metallothionein,[24,25] incorporate $Cd_3(\mu\text{-Cys-}S)_3$ rings. The exchange reaction (1) demonstrates the ease of replacement of M(II) by M(II)′ in bridged tetrahedral S_4 sites, over the substantial metal ion radius range of 0.72 (Co)–0.92 (Cd) Å. This type of substitution, albeit by different reactions but with the same metal ions, has been observed in a large number of metalloproteins,[49] including metallothionein.[26] Cobalt(II) thionein has been prepared by anaerobic reaction of Co(II) salts with the apoprotein,[26] and Zn(II) has been reported to displace Co(II) from the protein.[26b] Like other tetrahedral Co^{II}–S_4 complexes,[4,26b] $[Co_4(SPh)_{10}]^{2-}$ is a reasonable spectroscopic model of the protein chromophore. With use of intensity-weighted mean values for ν_3 (14 500 cm^{-1}) and ν_2 (7500 cm^{-1})[45,46] and a previous treatment,[4] the ligand field splitting parameter $\Delta_t = 4500$ cm^{-1} vs. 4780 cm^{-1} for the protein.[26b] The results of this investigation raise the possibility of metal ion substitution in other thiolate cage complexes, either by a reaction analogous to (1) or by

(42) Suzuki, K. T.; Maitani, T. *Experientia* **1978**, *34*, 1449. Sadler, P. J.; Bakka, A.; Beynon, P. J. *FEBS Lett.* **1978**, *94*, 315.
(43) Carson, G. K.; Dean, P. A. W.; Stillman, M. J. *Inorg. Chim. Acta* **1981**, *56*, 59.
(44) Observations i–iii, taken collectively, are consistent with the presence of only the species in Figure 1, but they cannot rigorously eliminate the possible formation (in minor amounts) of complexes with nuclearities other than 1 and 4.
(45) Spectra of $[Fe_4(SPh)_{10}]^{2-}$[28] and $[Co_4(SPh)_{10}]^{2-}$[16] are available elsewhere.
(46) For example, in the Co/Zn (Cd) systems these shifts of ν_3 maxima are observed as $f_{Co} = 1 \rightarrow 0.25$: 754–741 (748), 716–695 (692), 615–609 (607) nm. Because of these shifts intensity changes at λ_{max} (≲20%) are less significant than in the above cases. These and other absorption spectra were recorded at ~5 mM in total M(II).
(47) The volumes of the idealized Cd_4 tetrahedron and S_6 octahedron in $[Cd_4(SPh)_{10}]^{2-}$ are 34% and 14% larger, respectively, than those in $[Co_4(SPh)_{10}]^{2-}$.
(48) Blachnik, R.; Hoppe, A.; Rabe, U.; Wickel, U. *Z. Naturforsch., B: Anorg. Chem., Org. Chem.* **1981**, *36B*, 1493.
(49) Vallee, B. L.; Holmquist, B. *Adv. Inorg. Biochem.* **1980**, *2*, 27.

equilibration of the cage with mononuclear species. Unsymmetrical cages of nuclearity 3 and 4 that provide inequivalent, bridged $M^{II}(SR)_4$ sites with tetrahedral stereochemistry are a requisite step toward the simulation of the M(II) site aggregates in metallothionein.

Acknowledgment. This research was supported by NIH Grant GM 28856. NMR and X-ray diffraction equipment used in this research were obtained by NSF Grants CHE 80-00670 and CHE 80-08891. We thank J. M. Berg for the volume calculations in Table IV and Professor D. Coucouvanis for a preprint of ref 19.

Registry No. $(Me_4N)_2[Zn_2(SPh)_{10}]$, 76915-21-4; $(Et_4N)_2[Zn_4(SPh)_{10}]$, 82665-17-6; $(Et_4N)_2[Cd(SPh)_4]$, 82665-18-7; $(Me_4N)_2[Fe_4(SPh)_{10}]$, 74829-06-4; $[Fe_4(SPh)_{10}]^{2-}$, 74829-05-3; $[Co_4(SPh)_{10}]^{2-}$, 57659-25-3; $[Zn_4(SPh)_{10}]^{2-}$, 76915-20-3; $[Cd_4(SPh)_{10}]^{2-}$, 82665-19-8; $(Et_4N)_2[Cd_4(SPh)_{10}]$, 82665-20-1.

Supplementary Material Available: Crystal structure data for $(Me_4N)_2[Fe_4(SPh)_{10}]\cdot C_4H_7N$ including thermal parameters of the anion (Table S-I), positional and thermal parameters of the cations and solvate molecule (Table S-II), calculated H atom coordinates (Table S-III), and calculated and observed structure factors (Table S-IV) (39 pages). Ordering information is given on any current masthead page.

Contribution from the Institut für Anorganische Chemie and the Laboratorium für Kristallographie, Universität Bern, CH-3000 Bern 9, Switzerland

Syntheses and Crystal and Molecular Structures of Hexaaquaruthenium(II) *p*-Toluenesulfonate and Hexaaquaruthenium(III) *p*-Toluenesulfonate, $[Ru(H_2O)_6](C_7H_7SO_3)_2$ and $[Ru(H_2O)_6](C_7H_7SO_3)_3\cdot 3H_2O$

PAUL BERNHARD,[1a] HANS-BEAT BÜRGI,*[1b] JÜRG HAUSER,[1b] HANS LEHMANN,[1a] and ANDREAS LUDI*[1a]

Received March 22, 1982

Crystals of $Ru(H_2O)_6(tos)_2$ (II) (tos^- is *p*-toluenesulfonate) were grown from aqueous $Ru(H_2O)_6^{2+}$ solutions obtained by reduction of RuO_4 solutions with metallic lead. Crystals of $Ru(H_2O)_6(tos)_3\cdot 3H_2O$ (III) were grown from aqueous $Ru(H_2O)_6^{3+}$ obtained by oxidation of a $Ru(H_2O)_6^{2+}$ solution with O_2. For II the space group is $P\bar{1}$ with cell parameters a = 6.138 (1) Å, b = 7.287 (2) Å, c = 12.423 (4) Å, α = 92.22 (2)°, β = 94.82 (2)°, γ = 107.13 (2)°, and Z = 1. For III the space group is $C2/c$ with lattice constants a = 25.466 (7) Å, b = 7.235 (4) Å, c = 35.113 (8) Å, β = 93.97 (2)°, and Z = 8. The structure of II was refined to R = 3.3% for 2302 reflections with $F_o > \sigma(F_o)$; the structure of III, to R = 5.2% for 2989 reflections with $F_o > \sigma(F_o)$. In both structures $Ru(H_2O)_6$ octahedra are linked by hydrogen bonds to the SO_3 groups of the anion, the O-H···O distances ranging from ~2.5 to 3.0 Å. The average metal–oxygen distance is 2.122 (16) Å for Ru(II)–OH_2 and 2.029 (7) Å for Ru(III)–OH_2. The effect of the change in bond length on the rate of the $Ru(H_2O)_6^{3+/2+}$ self-exchange reaction is discussed.

Introduction

The coordination chemistry of ruthenium in oxidation states II and III is dominated by nitrogen donors.[2] The preparative chemistry as well as thermodynamic and kinetic properties for a broad range of ammine complexes has been thoroughly studied by Taube and his co-workers.[3] Many of these studies have been concerned with electron-transfer reactions, including self-exchange reactions. The comparison of these results with the behavior of first-row transition elements and the relationship between the electron-transfer kinetics and structural parameters continue to pose intriguing and sometimes puzzling problems.[4] In contrast to the wealth of information available for the ruthenium ammines, surprisingly few studies have dealt with the hexaaqua ions of ruthenium,[5-9] with most investigations confined to dilute solutions. The case of the ruthenium aqua ions deserves special attention since the pair $Ru(H_2O)_6^{3+}/Ru(H_2O)_6^{2+}$ is so far the only example of a low-spin t_{2g}^5–t_{2g}^6 redox couple within the metal aqua ions. Of prime interest, again, are the self-exchange reaction and the connection of the corresponding kinetic parameters to the molecular structure. The application of the Marcus cross relation to a series of redox reactions involving either $Ru(H_2O)_6^{3+}$ or $Ru(H_2O)_6^{2+}$ led to an estimate of 60 ± 40 M^{-1} s^{-1} for the rate constant of the self-exchange reaction. Sutin concluded from these data that there exists a difference of approximately 0.1 Å between the ruthenium–oxygen bond lengths in the two aqua ions.[8] We therefore focused our efforts on isolating and investigating crystalline salts of $Ru(H_2O)_6^{3+}$ and $Ru(H_2O)_6^{2+}$. A special bonus of these efforts resulted for the preparative inorganic chemist: the availability of a stable solid salt of $Ru(H_2O)_3^{2+}$ as a starting material opens up new and facile synthetic routes to a variety of ruthenium complexes.[10]

Experimental Section

A. Preparations. $Ru(H_2O)_6^{2+}$. The $Ru(H_2O)_6^{2+}$ solutions prepared according to Kallen and Earley[7] contained substantial amounts of tin, as was shown by atomic absorption spectroscopy. We therefore used a different synthetic procedure: A 1.5-g sample of Ru metal was fused in a Ni crucible with 30 g of KOH. A 3-g amount of

(1) (a) Institut für Anorganische Chemie. (b) Laboratorium für Kristallographie.
(2) Cotton, F. A.; Wilkinson, G. "Advanced Inorganic Chemistry", 4th ed.; Interscience: New York, 1980; Chapter 22-F.
(3) Taube, H. *Comments Inorg. Chem.* **1981**, *1*, 17.
(4) Sutin, N. *Tunneling Biol. Syst. [Proc. Symp.] 1977* **1979**, 201.
(5) Cady, H. H.; Connick, R. E. *J. Am. Chem. Soc.* **1958**, *80*, 2646.
(6) Mercer, E. E.; Buckley, R. R. *Inorg. Chem.* **1965**, *4*, 1692.
(7) Kallen, T. W.; Earley, J. E. *Inorg. Chem.* **1971**, *10*, 1149.
(8) Böttcher, W.; Brown, G. M.; Sutin, N. *Inorg. Chem.* **1979**, *18*, 1447.
(9) Harzion, Z.; Navon, G. *Inorg. Chem.* **1980**, *19*, 2236.
(10) Bernhard, P.; Lehmann, H.; Ludi, A. *J. Chem. Soc., Chem. Commun.* **1981**, 1216.

0020-1669/82/1321-3936$01.25/0